CLEAVAGE FRACTURE OF A HIGH STRENGTH STEEL WELD METAL

R K HUGHES and J C RITTER
DSTO Aeronautical and Maritime Research Laboratory
PO Box 4331, Melbourne, VIC. 3001, Australia

ABSTRACT

Cleavage fracture resistance and fracture micromechanisms have been investigated in a high strength multiple-pass weld metal deposited by the flux cored arc process. Notched specimens were broken in slow four-point bending to evaluate the critical tensile stress for cleavage initiation. Detailed examination of fracture surfaces by scanning electron microscopy revealed the important role of inclusions in acting as cleavage initiation sites. A basic flux wire filler resulted in a significantly lower inclusion volume fraction and superior impact toughness compared with a rutile flux, but little change occurred in inclusion size distribution or cleavage resistance. The effective surface energy of fracture was calculated using a modified Griffith equation for a penny shaped crack and found to be in close agreement with previously published values.

KEYWORDS

Cleavage fracture, weld metal, inclusions.

INTRODUCTION

While high strength steels have been satisfactorily joined by all of the conventional arc welding processes, concern has been shown over the ability of weld metal deposited by the flux cored arc (FCA) process to achieve consistently high levels of toughness. In a recent comparison of manual metal arc (MMA), submerged arc (SA) and FCA weld metals at yield stress of approximately 700 MPa, Zhou (1995) found that FCA weld metal delivered inferior CTOD fracture toughness. It has also been noted (Dixon and Ritter 1986) in the explosion bulge testing of welds joining 550 MPa yield stress steel that while gas metal arc, MMA and SA processes could all produce acceptable welds, the FCA process was regarded as unsatisfactory.

In this work, FCA weld metal joining a 690 MPa yield stress naval construction steel has been studied to examine the influence of flux system on inclusion population and microstructure, and their combined effect on weld metal toughness. The flux system may be classified as either basic or rutile depending on the major constituents. A basic flux will contain calcium carbonate and calcium fluoride as the major ingredients while rutile fluxes include titanium dioxide and silica.

Basic fluxes are associated with excellent mechanical and toughness properties but they typically possess inferior arc stability which can make positional welding difficult. Resistance to cleavage fracture was measured for weld metal belonging to both flux systems by low temperature notch bend testing and impact toughness was assessed by the Charpy technique.

Many investigations have shown that inclusions or other second-phase particles can provide a crack nucleus for cleavage fracture initiation in weld metals (Tweed and Knott, 1983; McRobie and Knott, 1985; Bowen *et al.*, 1986; Bose *et al.*, 1995). A model proposed by Tweed and Knott (1983) for cleavage fracture in C-Mn weld metals identified localised plasticity in grain boundary ferrite as leading to the cracking of non-metallic inclusions at low overall strains, with cleavage fracture then initiated at cracked inclusions at some critical local fracture stress. The critical role of non-metallic inclusions of diameters greater than 0.9μm in controlling cleavage fracture was confirmed for $2^1/_4$ Cr-1Mo weld metal (Bowen *et al.*, 1986). It was found that the initiation sites were situated close to the position of the peak tensile stress ahead of the crack tip, confirming that cleavage fracture was controlled by the maximum tensile stress.

EXPERIMENTAL PROCEDURE

Multiple-pass welds were deposited with cored wires of basic and rutile classifications. Welding parameters and pass sequence were representative of those employed when joining high strength, quenched and tempered, naval construction steels. The chemical compositions are given in Table 1.

Table 1 Chemical analysis of weld metal, wt %.

Flux	C	Mn	Si	S	P	Ni	Cr	Mo	Ti	B	N	O
Basic	.04	1.02	.47	.012	.017	2.82	.02	.27	.03	.0018	.0053	.045
Rutile	.06	1.76	.23	.010	.011	2.64	.03	.01	.03	.0025	.0104	.045

Notch bend testing was performed to measure (i) the maximum tensile stress below a notch at failure, being the cleavage fracture strength, σ_F, and (ii) the local cleavage fracture stress (or critical local tensile stress), σ_f^*, at the point of cleavage initiation. Blunt notch, or single-edge-notch-bend (SENB), test specimens were prepared with geometry similar to that analysed by Griffiths and Owen (1971). The technique employs an elastic-plastic finite-element analysis (FEA) to describe the stress-strain distribution ahead of a blunt notch in a SENB specimen tested in slow, four-point bending. The FEA program used to calculate this distribution was ANSYS 5.1 with work hardening properties included by defining stress and strain values, which corresponded to a power curve relation, in the plastic region. Fracture micromechanisms were investigated by analysing the stress and strain distribution in the specimen at fracture. Testing was performed at -150 and -170°C in order to ensure that cleavage fracture occurred at, or before, the onset of general yield. The uniaxial yield stress, σ_y, was determined at the same temperatures in a separate tensile test.

Fracture surfaces of broken SENB specimens were examined by scanning electron microscope (SEM) in order to identify the cleavage initiation site. If a cracked or decohered particle was found at the initiation site by tracing diverging river lines on a cleavage facet, particle size and its distance below the notch root were measured. Energy-dispersive X-ray analysis (EDX) equipment attached to the SEM was used for qualitative chemical analysis of particles.

Inclusion size measurements were taken on carefully prepared weld metal sections and the corresponding three dimensional particle distributions were calculated using the Johnson-Saltykov method as described by Underwood (1970).

Standard Charpy specimens were taken transverse to the direction of welding, in the same orientation as for the SENB specimens, and tested over the temperature range 21 to -107°C. The ductile to brittle transition was taken to be the point of the 50% fracture appearance transition temperature (FATT).

RESULTS

Weld metal microstructures were complex mixtures of as-deposited and reheated constituents which included acicular ferrite, proeutectoid ferrite with ferrite side-plate and ferrite-carbide aggregate. The basic flux resulted in a coarser structure with more grain boundary ferrite and less acicular ferrite, despite the weld metal being deposited at a slightly lower heat input.

The results of notch bend testing and fracture initiation details are shown in Table 2, where d is the inclusion diameter and X_0 is the distance from the notch root to the initiation site. The distance from the notch root to the peak in the stress distribution is given as X^{max}. Initiation location is compared with the location of peak stress by the ratio X_0:X^{max} and initiation is deemed to have occurred in the region of peak stress if X_0 is located within +/- 20% of X^{max}. Test specimens are identified according to the coupon from which they were taken and their location within the weldment by the following system:

BT Basic flux, specimen from top of half K preparation weldment.
BB Basic flux, specimen from bottom of half K preparation weldment.
RA Rutile flux, specimen from side 1 of double V preparation weldment.
RB Rutile flux, specimen from side 2 of double V preparation weldment.

Table 2 Results of notch bend testing and fracture initiation details.

Specimen	Temp (°C)	σ_y (MPa)	σ_F (MPa)	X^{max} (μm)	d (μm)	X_0 (μm)	X_0: X^{max}	σ_f^* (MPa)
Basic Flux								
BT1	-170	840	2356	393	2.4	850	>	2085
BT2	-170	840	2270	394	2.3	680	>	2065
BT3	-170	840	2246	391	4.1	420	=	2234
BT4	-170	840	2207	393	1.5*	400	=	2203
BT5	-170	840	2187	390	1.8	420	=	2169
BB1	-170	904	2581	464	3.2*	950	>	2247
BB2	-170	904	2465	393	4.5	790	>	2162
Rutile Flux								
RA1	-150	904	2428	393	1.2	280	<	2339
RA2	-150	904	2378	394	3.2	570	>	2228
RA3	-170	937	2336	326	1.2	560	>	2092
RA4	-170	937	2278	323	1.0*	300	=	2264
RB1	-170	850	2286	394	1.4	410	=	2279
RB2	-170	850	2224		RU			
RB3	-170	850	2160	329	NI	520	>	2031

RU = Region of initiation unclear; NI = No inclusion at initiation site; * = Inclusion decohered

In twelve of the fourteen specimens it was possible to identify a single and distinct non-metallic inclusion, of 1.0 μm or greater in diameter, which had initiated cleavage. Nine inclusions had cracked and three had decohered from the surrounding matrix. A cracked inclusion on a large cleavage facet at the initiation site is shown in Fig. 1. In two specimens it was either not possible to identify the region of initiation or no inclusion was found at the initiation site.

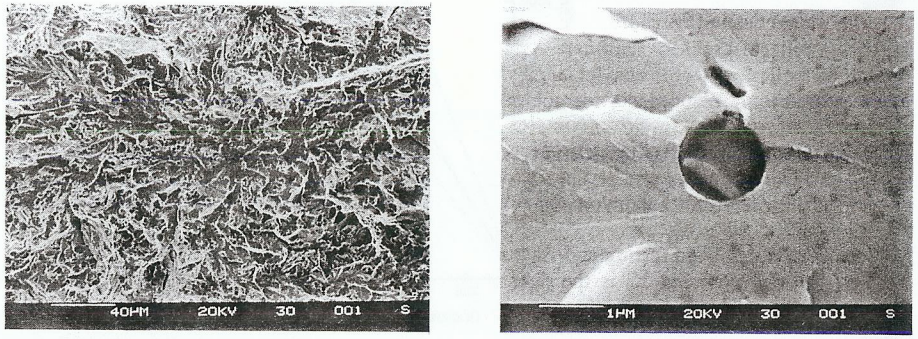

Fig. 1 Region of cleavage initiation and cracked inclusion at the initiation site.

The stress distribution below the notch root at failure as calculated by FEA is shown in Fig. 2 for the four test specimens in the RA series. The location of fracture initiation is marked on each distribution.

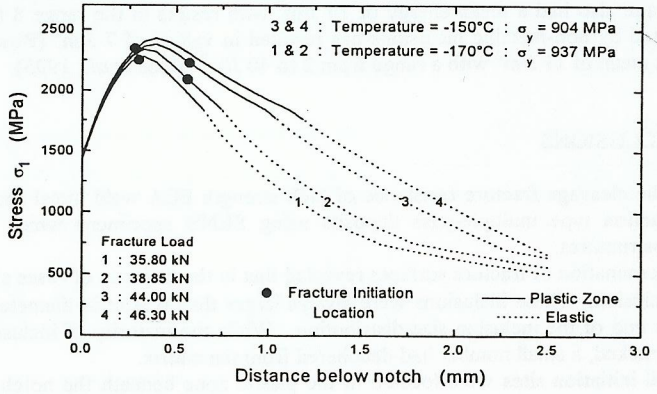

Fig. 2 Distribution of stress below the notch root at fracture; RA series specimens.

The parameters of the inclusion size distributions and calculated volume fractions of weld metal occupied by inclusions are listed in Table 3. While inclusion sizes at the distribution parameters were only slightly larger in weld metal deposited with the rutile flux, the inclusion volume fraction was significantly higher. Oxygen content, given with the chemical compositions in

Table 1, failed to provide a measure of the higher inclusion population associated with the rutile flux.

Table 3 Inclusion size distribution parameters and volume fraction.

Flux	Median dia. (μm)	90th percentile (μm)	95th percentile (μm)	99th percentile (μm)	Vol. Fract. (%)
Basic	0.30	0.56	0.64	1.19	0.27
Rutile	0.38	0.76	0.92	1.46	0.58

DISCUSSION

Established theories of cleavage fracture in mild steels predict that failure will occur when a critical tensile stress is locally exceeded (Wilshaw *et al.*, 1968; Ritchie *et al.*, 1973). If this applies to the high strength FCA weld metal in the current investigation it would be expected that the cleavage initiation site will be approximately coincident with X^{max}. The exact location of initiation will however depend on the probability of a sufficiently large stress encountering an inclusion of sufficient size to provide a pre-crack for cleavage, rather than necessarily occurring at the peak stress location. Of the thirteen initiation sites identified, five were in the region of peak stress, seven were deeper below the notch and in only one specimen did initiation occur closer to the notch than the region of peak stress. Attainment of a critical level of imposed strain is therefore unlikely to be of importance in the cleavage fracture of these weld metals because high levels of plastic strain are only encountered close to the notch tip.

The mean diameter of inclusions initiating cleavage was 2.3μm which places them at the upper end of the size distribution. Analysis by EDX established that these inclusions contained appreciable amounts of Ti and Mn indicating that they resulted from deoxidation product. Both welds also contained a few larger inclusions in the size range 5 to 10μm which had not acted as cleavage initiation sites. These were found to contain appreciable amounts of Ca or Si for the basic and rutile fluxes respectively. These qualitative indications are consistent with the expected major constituent elements in slag entrapment inclusions which had failed to separate to the weld bead surface.

Inability of the largest particles to initiate cleavage has also been observed by Linaza *et al.* (1995) in forging steels in which TiN particles of approximately 2μm in size were found to initiate cleavage while larger TiN particles of over 6μm were present but did not participate in cleavage initiation. This behaviour, which reflects that of the inclusion particles in FCA weld metal, was attributed to two possible causes. The first suggests that larger particles can break at lower stresses than small particles due to a Weibull volume effect. If, therefore, cracks are nucleated in large particles while local stress is too low to promote propagation of the crack across the particle-matrix interface, cracks will blunt at the interface and will not subsequently cause final cleavage failure. A further possible reason is that the very small number of the largest particles reduces the possibility of their being encountered in the zone of maximum tensile stress ahead of the notch in a SENB specimen taken from the material. The compositional difference in the largest inclusions in the FCA weld metal introduces another possibility that slag entrapment has greater resistance to cracking or decohesion from the matrix compared to the deoxidation product.

The yield stress and local cleavage fracture stress of the two FCA weld metals are compared in Table 4. Specimens from the top of the half K (basic flux) coupon are compared with specimens from side 2 of the double V (rutile flux) coupon, and the bottom of the half K is compared with side 1 of the double V coupon. In this way, the initial passes of weld metal at the bottom of the half K and on side 1 of the double V, which may have strain aged when later weld passes solidified and cooled, are separated from weld metal which was not subjected to potential strain ageing. The weld metals possessed very similar yield stress and cleavage fracture resistance at the locations of comparison, despite the significant difference in inclusion volume fraction.

Table 4 Yield stress at -170°C and average local cleavage fracture stress.

Flux	σ_y (MPa)	σ_f* (MPa)	σ_y (MPa)	σ_f* (MPa)
	Top		Bottom	
Basic	840	2151	904	2205
	Side 2		Side 1	
Rutile	850	2155	937	2231

The FATT parameter is compared for the two weld metals in Table 5. The basic flux resulted in a lower transition temperature and generally high impact energies indicating superior impact toughness compared with the weld metal deposited by the rutile flux wire.

Table 5 Fracture appearance transition temperature.

Flux	FATT (°C)	FATT (°C)
	Top	Bottom
Basic	-41	-32
	Side 2	Side 1
Rutile	-31	-24

While the basic flux wire resulted in weld metal with superior impact toughness, the cleavage resistance of both weld metals measured in slow four-point bending was virtually identical. This contradiction is explained by the different fracture micromechanisms operating in the two test techniques. Failure of Charpy specimens in the transition region involves significant plasticity and occurs after microvoid nucleation and coalescence. Weld metal deposited by a rutile flux wire has a significantly larger volume fraction of inclusions and this will result in a greater density of microvoids and a lower true strain to fracture. Cleavage initiation, in contrast, occurs at a single large inclusion. Inclusion size distribution will therefore replace volume fraction as the factor controlling cleavage because a single large inclusion will be sufficient to provide a microcrack to initiate fracture. Weld metal deposited with basic and rutile fluxes had very similar inclusion size distributions which consequently resulted in a very similar cleavage fracture resistance, despite the lower volume fraction associated with the basic flux.

Values of local cleavage fracture stress are plotted against the reciprocal square root of inclusion diameter in Fig. 3. The effective surface energy was calculated for all specimens using the modified Griffith equation from Curry and Knott (1978) which relates the stress necessary to propagate a penny shaped crack into the surrounding ferrite matrix, to microcrack size. The mean effective surface energy of 15 J/m^2 was in close agreement with previously published

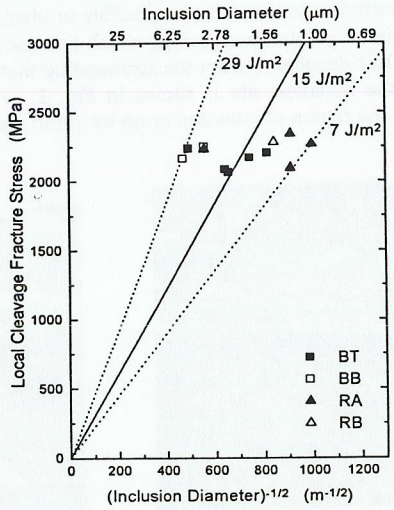

Fig. 3 Local cleavage fracture stress versus the reciprocal square root of inclusion diameter.

values for steels and weld metals. Investigating cleavage fracture in steels containing distributions of spheroidised carbides, Curry and Knott (1978) correlated local cleavage fracture stress with the 95th percentile carbide radius and obtained an effective surface energy of 14 J/m^2. Forging steels investigated by Linaza et al. (1995) in which TiN particles initiated cleavage also had a mean energy of 14 J/m^2 with results in the range 8 to 20 J/m^2. Cleavage initiated by non-metallic inclusions has resulted in values of 7 J/m^2 (Bowen and Knott, 1988) and a mean of 11 J/m^2 with a range from 2 to 40 J/m^2 (Bose *et al.*, 1995).

CONCLUSIONS

1. The cleavage fracture resistance of high strength FCA weld metal has been investigated in production type multiple-pass deposits using SENB specimens which sampled a range of microstructures.
2. Examination of fracture surfaces revealed that in the majority of cases cleavage initiated from an inclusion. These inclusions were always larger than 0.9μm in diameter placing them at the upper end of the inclusion size distribution. While the majority of inclusions at initiation sites had cracked, a small number had decohered from the matrix.
3. All initiation sites were located in the plastic zone beneath the notch with the majority of sites in the region of peak stress or deeper beneath the notch, indicating that cleavage fracture is dependent on a critical level of imposed tensile stress.
4. The inclusions initiating fracture invariably came from deoxidation product. A sparse population of much coarser inclusions approaching or exceeding 10μm in size arising from slag entrapment played no role in cleavage initiation.

5. Weld metal deposited with a basic flux system wire had a significantly lower inclusion volume fraction compared to weld metal deposited with a rutile flux system wire. Both welds had similar inclusion size distributions. The local cleavage fracture stress was very similar in the two weld metals despite the difference in inclusion volume fraction because a single large inclusion will be sufficient to provide a microcrack to initiate fracture.
6. A modified Griffith equation may be used to equate the size of the inclusions initiating cleavage with the local cleavage fracture stress, and thereby determine the effective surface energy. The mean effective surface energy of 15 J/m^2 was in close agreement with previously published values for steels and weld metals.

ACKNOWLEDGEMENTS

Dr J. L. Davidson is thanked for assisting with the theory and analysis of the particle size distributions, A. Debicki for finite element analysis and J. Russell for scanning electron microscopy.

REFERENCES

Bose, W. W., P. Bowen and M. Strangwood (1995). Cleavage fracture in high strength low alloy weld metal. *4th Int. Conf. on Trends in Weld. Res.*, Gatlinburg, Tennessee, 5-8 June.

Bowen, P., M. B. D. Ellis, M. Strangwood and J. F. Knott (1986). Micromechanisms of brittle fracture in $2^1/_4$Cr-1Mo weld metal. *Proc. Conf. ECF6, Vol.III*, 1751-1762.

Bowen, P. and J. F. Knott (1988). Micromechanisms of brittle fracture related to local brittle zone assessment. *7th Int. Conf. on Offshore Mech. and Arctic Eng.*, Houston, Texas, 7-12 February, 503-507.

Curry, D. A. and J. F. Knott (1978). Effects of microstructure on cleavage fracture stress in steel. *Metal Science*, **12**, 511-514.

Dixon, B. F. and J. C. Ritter (1986). Welding of quenched and tempered steels for submarine construction. *34th National Conf. of the Australian Welding Inst.*, 319-332.

Griffiths, J. R. and D. R. J. Owen (1971). An elastic-plastic stress analysis for a notched bar in plane strain bending. *J. Mech. Phys. Solids*, **19**, 419-431.

Linaza, M. A., J. L. Romero, J. M. Rodriguez-Ibabe and J. J. Urcola (1995). Cleavage fracture of microalloyed forging steels. *Scripta Metall. et Mater.*, **32**, 395-400.

McRobie, D. E. and J. F. Knott (1985). Effects of strain and strain ageing on fracture toughness of C-Mn weld metal. *Mat. Sci. and Tech.*, **1**, 357-365.

Ritchie, R. O., J. F. Knott and J. R. Rice (1973). On the relationship between critical tensile stress and fracture toughness in mild steel. *J. Mech. Phys. Solids*, **21**, 395-410.

Tweed, J. H. and J. F. Knott (1983). Effect of reheating on microstructure and toughness of C-Mn weld metal. *Metal Science*, **17**, 45-54.

Underwood, E. E. (1970). *Quantitative Steriology*. Addison-Wesley, Reading, Massachusetts.

Wilshaw, T. R., C. A. Rau and A. S. Tetelman (1968). A general model to predict the elastic-plastic stress distribution and fracture strength of notched bars in plane strain bending. *Eng. Fract. Mech.*, **1**, 191-211.

Zhou, Z. (1995). CTOD fracture toughness and microstructure of high strength steel welds. *Svetsaren*, **50**, 26-28.